Korean J. Chem. Eng., 35(1), 246-250 (2018)
DOI: 10.1007/s11814-017-0243-6

pISSN: 0256-1115
eISSN: 1975-7220

Effects of growth temperature on titanium carbide (TiC) film formation using low-frequency (60 Hz) plasma-enhanced chemical vapor deposition

Hong Tak Kim*, Sung-Youp Lee, Hyeong-Rag Lee**, and Chinho Park*,†**

*School of Chemical Engineering, Yeungnam University, Gyeongsan 38541, Korea
**Department of Physics, Kyungpook National University, Daegu 41566, Korea
(*Received 23 May 2017 • accepted 5 September 2017*)

Abstract−TiC films were formed by low-frequency (60 Hz) plasma-enhanced chemical vapor deposition (LF-PECVD) using $TiCl_4$, CH_4, and H_2 gas mixtures. The effects of the growth temperature and feasibility for the on-glass deposition of TiC films were investigated. The growth kinematics of TiC films was controlled mainly by surface-reactions below 450 °C, and dominated by a mass-transfer process above 450 °C. The films exhibited a face-centered cubic structure, and the preferred orientation of film growth was mainly the (200) plane. The [C]/[Ti] ratio was over-stoichiometric below 400 °C, and became almost stoichiometric above 450 °C. The optical properties of the films were characterized by high reflectance in near infrared (NIR) region and a steep edge in the visible region, and the reflectance in the NIR region increased gradually with increasing temperature. As a result, LF-PECVD is a useful technique to acquire Cl-free TiC films at relatively low temperatures.

Keywords: Low-frequency, PECVD, Plasma, Titanium Carbide, TiC

INTRODUCTION

Titanium carbide (TiC) films have extremely high strength, high melting point, good heat-resistance, good electrical conductivity, and high chemical stability [1,2]. Consequently, they are used widely as abrasion-resistant coatings, heater-shields, decorative films, and supercapacitors [1-3]. Usually, the well-known chemical vapor deposition reactions for the formation of TiC films proceed according to following equation [4,5]:

$$TiCl_4+CH_4 \rightarrow TiC+4HCl \quad (1)$$

This chemical reaction is thermodynamically favored at temperatures above 900 °C, but this limits the substrate selection and device applications. The plasma process is useful for reducing the growth temperature for film formation because the plasma discharge can easily generate ions and reactive radicals [6,7]. Generally, DC and high frequency power sources are applied to generate a plasma discharge. The commercial frequency (50 or 60 Hz) is not used in film deposition because of the low-deposition yields caused by the noncontinuous but discrete plasma discharge. On the other hand, a low-frequency (LF) discharge has peculiar characteristics, such as relatively high electron temperature and low surface damage [8,9]. In particular, the relatively high electron temperature of the LF-discharge makes it possible to produce more active radicals, which leads to film formation under low temperature conditions [10,11]. In addition, the LF-power source has a very simple structure in a circuit, as shown in Fig. 1, and it is made up of inexpensive electrical components. Therefore, the LF-power source can be easy to make at low cost, which is suitable for plasma experiments on a laboratory scale. The comparisons of the characteristics of the plasma generated by LF, DC, and RF power sources are summarized in Table 1 [11].

In this study, TiC films were deposited on glass substrates by LF plasma-enhanced chemical vapor deposition (PECVD) using titanium chloride ($TiCl_4$), hydrogen (H_2), and methane (CH_4) gas mixtures. The effects of the growth temperature for the TiC film formations were investigated. In particular, we focused on the chemical kinematics of the growth process and the feasibility for on-glass deposition.

EXPERIMENTAL DETAILS

TiC films were formed on soda-lime glass substrates (2 cm×2 cm) by a low-frequency (60 Hz) PECVD method, and deposited at different deposition temperatures to study the effects of the growth temperature. The reaction chamber was a stainless steel vessel with a diameter of 40 cm and a height of 46 cm. The disk electrodes were made of stainless steel with a 12 cm diameter, separated by a 5 cm gap. The substrate was placed on the bottom electrode with a heating unit, and the substrate temperature was controlled in the range of 350-550 °C using a heating control unit (Autonics, TZ4M). Prior to film deposition, the reaction chamber was evacuated to a base pressure of 0.67 Pa by a mechanical pump, and the substrate temperature was heated to the desired temperature. The precursor gases were introduced into the reaction chamber, and a low-frequency power of 35 W (340 V, 103 mA) was applied to generate the plasma discharge. The H_2, CH_4, and $TiCl_4$ gases (Aldrich, 99.9%) were used as precursors, and argon (Ar) was used as a carrier gas for the liquid $TiCl_4$. The gas partial pressures of H_2 (49.3 Pa), and CH_4 (9.33 Pa) were regulated by using a micro-needle valve

†To whom correspondence should be addressed.
E-mail: chpark@ynu.ac.kr

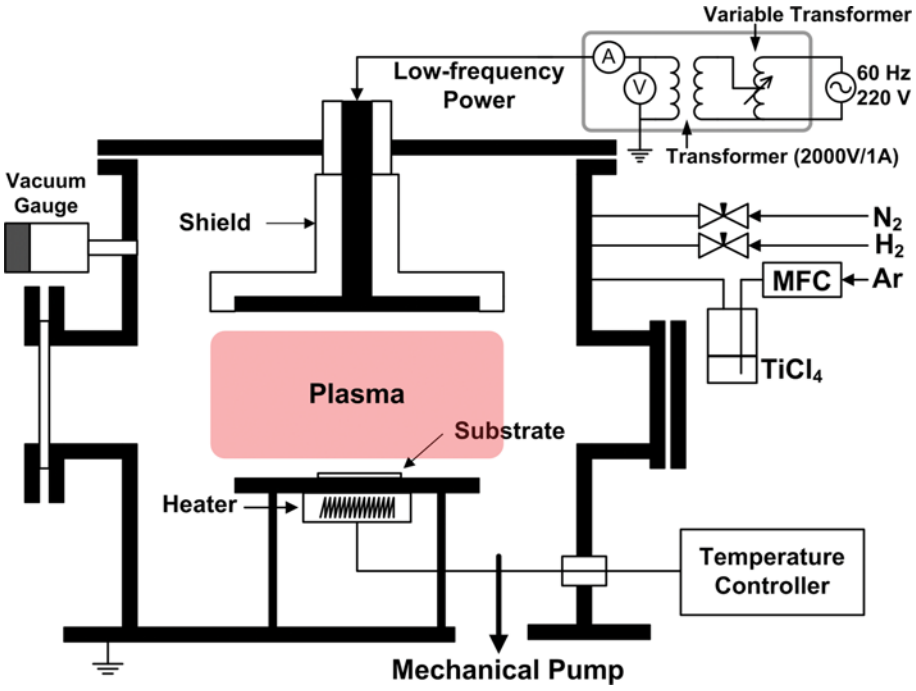

Fig. 1. Schematic diagram of the experimental setup for TiC film deposition using low-frequency (60 Hz) plasma-enhanced chemical vapor deposition.

Table 1. Comparison for the characteristics of the plasma generated by low-frequency (LF), direct current (DC), and radio-frequency (RF) power sources

	LF	DC	RF
Power frequency	50/60 Hz	0	13.56 MHz
Ionization mode	γ-Mode	γ-Mode	α/γ-Mode
Discharge mode	Bipolar pulse	Continuous	Continuous
Electron temperature	Relatively higher than DC/RF		
Electron density	Relatively lower than DC/RF		
Energy loss	Lower than RF, similar to DC		
Deposition rate	Lower than DC/RF		
Metal deposition	Possible	Possible	Possible
Non-metal deposition	Possible	Difficult	Possible

Table 2. Properties of TiC films grown on soda-lime glasses using low-frequency (60 Hz) PECVD according to the deposition temperatures

Value	Deposition temperature (°C)				
	350	400	450	500	550
Deposition rate (nm/h)	45	60	87	91	92
Phase	TiC, TiO_2	TiC, TiO_2	TiC	TiC	TiC
Preferred orientation	(200)	(200)	(200)	(200)	(200)
Grain size (nm)	3.72	13.5	17.0	18.9	25.8
Ratio of C/Ti	1.39	1.12	0.94	1	1.02
Ratio of O/Ti	0.36	0.30	0.24	0.17	0.15
Ratio of Cl/Ti	0.028	0.012	0.004	0	0
Reflectance (@1500 nm) (%)	39.8	43.9	48.3	51.7	58.1

(Whitey, SS-22RS4) and the pressure of $TiCl_4$-Ar (1.33 Pa) was controlled with a mass flow controller (MFC, KOFLOC 3660). The bubbler of the $TiCl_4$ liquid was kept at room temperature and the flow rate of the Ar carrier gas was 2 sccm. The pressure of the gases was measured by capacitance manometer (MKS Baratron Type 122BA) and penning gauge (Varian 525). Fig. 1 presents a sche-

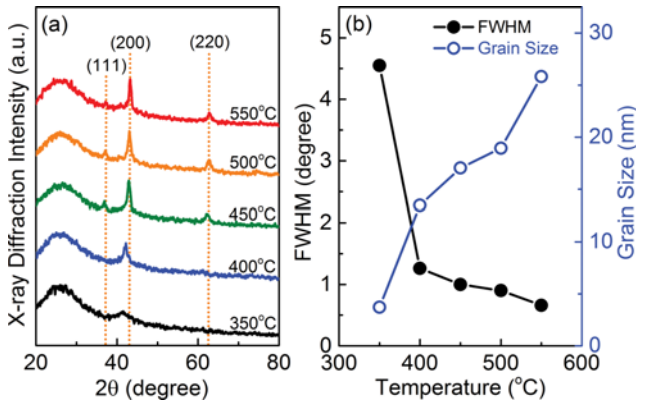

Fig. 2. (a) X-ray diffraction patterns of TiC films, and (b) FWHM of (200) plane and grain size of TiC films according to the deposition temperatures.

matic diagram of low-frequency (60 Hz) PECVD for TiC film formation.

The thickness and surface morphology of the TiC films were measured by scanning electron microscopy (SEM, Hitachi S-4100) with a voltage of 15 kV. The structural properties of the TiC films were identified by X-ray diffraction (XRD, Philips X'pert) using Cu Kα radiation (0.1541 nm) with a current and voltage of 30 mA and 40 kV, respectively, and the measurements were taken in the range, $20^{\circ} \leq 2\theta \leq 80^{\circ}$, in $\theta/2\theta$ mode with a scanning step of 0.01°. The optical properties of the films were measured by UV-Vis-NIR spectrophotometer (Varian CARY 5G) and compositional analysis of the TiC films was by X-ray photo-electron spectroscopy (XPS, VG Microtech MT-500) using Al Kα radiation (1486.6 eV) with a current of 3 mA and a voltage of 12 kV.

RESULTS AND DISCUSSION

Fig. 2(a) shows XRD patterns of the TiC films according to the deposition temperatures. The main peaks were observed at 38°, 42° and 62° 2θ, which were assigned to the (111), (200), and (220) planes, respectively. The crystal structure of the TiC films was NaCl-type with a face-centered cubic structure (JCPDS Card no. 65-8417). The (200) peak at a deposition temperature of 350 °C and 400 °C exhibited mixed phases of TiC and TiO_2, and the phase of TiO_2 originated from the surface oxidation of TiC films under atmospheric conditions (see the supplementary materials). The TiO_2 phase disappeared above 450 °C, which indicated the formation of stable TiC films. The grain size of the TiC films was calculated using Scherrer's equation [12,13], and the size increased from 3 nm to 27 nm with increasing growth temperature, as shown in Fig. 2(b). Fig. 3 shows SEM images of TiC films at different deposition temperatures. A rough surface morphology due to oxidation was observed at 350 °C, and the grain size increased gradually with increasing growth temperature. Fig. 4 shows the atomic concentration ratio of C, O, and Cl in reference to Ti. The [C]/[Ti] ratio was higher than the stoichiometric value at 350 °C and 400 °C, whereas the ratio of [C]/[Ti] became stoichiometric ratio above 450 °C. In addition, no chlorine component was detected in TiC films above 500 °C. The residual chlorine component in the TiC film could react with

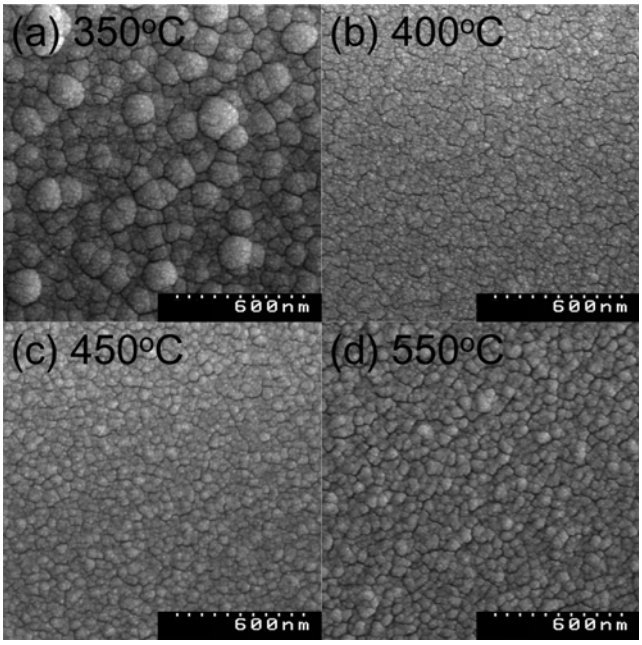

Fig. 3. Surface morphological SEM images of TiC films at different deposition temperatures.

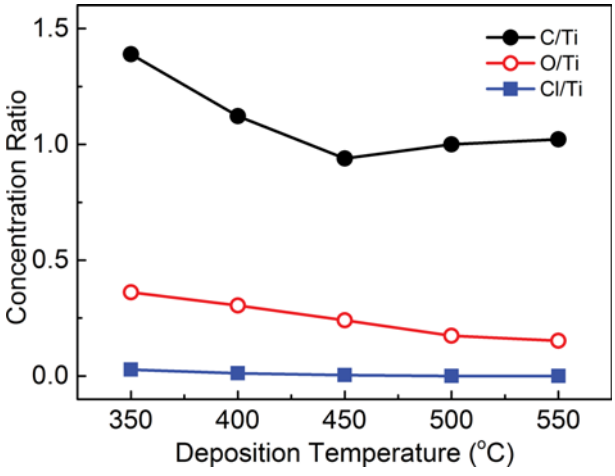

Fig. 4. Atomic compositional ratio of [C]/[Ti], [O]/[Ti], and [Cl]/[Ti] according to the deposition temperatures.

water vapor when exposed to the atmosphere, and form the undesirable adducts such as HCl and TiO_2 [14]. These adducts could damage the TiC films and the other layer in devices.

Fig. 5 shows the deposition rate of the TiC films at different growth temperatures. The deposition rate increased rapidly to 450 °C and the rate saturated above growth temperatures. The activation energy for the film deposition reaction was calculated from the Arrhenius plot of the deposition rate versus the inverse of temperature, and the Arrhenius's relation is given by [15,16]:

$$r = A\exp\left(-\frac{E_a}{RT}\right) \quad (2)$$

where r is the deposition rate, A is the frequency factor, E_a is the activation energy, R is the gas constant, and T is the absolute tem-

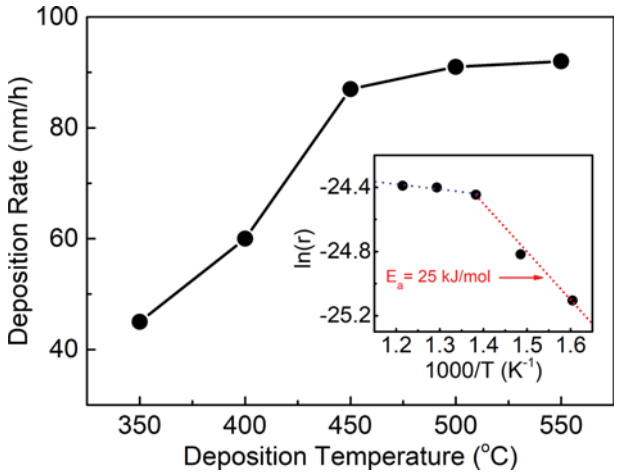

Fig. 5. Deposition rate (r) of TiC films at different deposition temperatures (inset: Arrhenius plot of ln(r) versus T^{-1}).

perature. E_a was estimated from the slope of the straight line in the ln(r)−(1/T) plot. Fig. 5 (inset) presents the Arrhenius plot of the deposition rate versus the inverse of temperature. The calculated E_a values were approximately 25 kJmol^{-1} below 450 °C, which was attributed to the surface-reaction limited regime [17]. These results suggest that film growth was controlled mainly by surface reactions rather than a mass transfer process at the low temperature region. Therefore, the rate of film growth is sensitive to the temperature, and the rate increased with increasing temperature. On the other hand, the growth rate was relatively independent of temperature above 450 °C, which means that the growth rate is controlled mainly by a mass transfer process. Generally, mass transport to the substrates is limited mostly by the external settings of reactor, such as flow rate, pressure, and reactor size.

Fig. 6 shows the reflectance spectra of the TiC films grown at different deposition temperatures. The optical properties of the TiC films were characterized by high reflectance in the near infrared (NIR) region, which was a typical property for metallic materials. The reflectance in the NIR region increased gradually with increasing temperature, which was closely related to the enhancement of metallic behavior of TiC films, due to a decrease in the concentration of O and Cl in the TiC films. In addition, absorption and a steep edge in a visible region were observed, which could be explained by the partial density of state and atomic selection rules [18]. The properties of TiC films according to the deposition temperatures were summarized in Table 2.

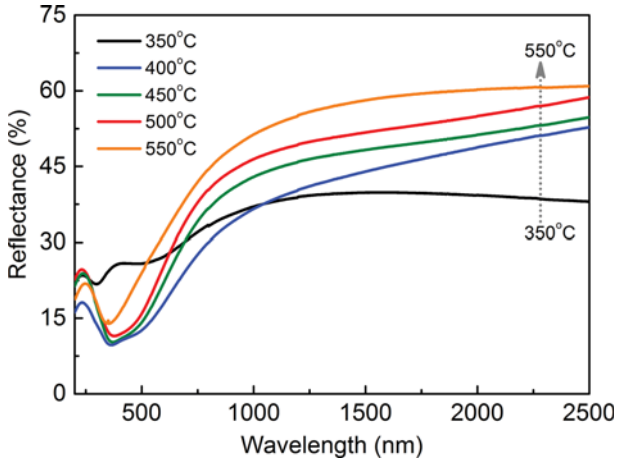

Fig. 6. Reflectance spectra of TiC films at different deposition temperatures.

CONCLUSION

TiC films were formed on soda-lime glass substrates by low-frequency (60 Hz) PECVD, and deposited at different deposition temperature to examine the effects of the growth temperature. H_2, CH_4, and $TiCl_4$ were used as the precursors and argon (Ar) as the carrier gas for the $TiCl_4$ liquid. The as-formed TiC films represented an NaCl-type with a face-centered cubic structure, and the preferred orientation of film formations was mainly the (200) plane. The [C]/[Ti] ratio exhibited higher values than 1 at 350 °C and 400 °C, and the [C]/[Ti] ratio reached the stoichiometric ratio above a growth temperature of 450 °C. In addition, no Cl was detectable above 500 °C. The reflectance in the near infrared (NIR) region increased gradually with increasing temperature, and a blue-shift of the reflectance edge was observed. The optical properties of the TiC films were characterized by high reflectance in the NIR region and a steep edge in the visible region. The growth of TiC films was controlled by a surface reaction process below 450 °C, while a mass-transfer process was more dominant than surface-reaction process above 450 °C. As a result, LF-PECVD developed in this study is a useful technique for acquiring Cl-free TiC films at relatively low temperatures. In addition, the LF power source is inexpensive and easy to produce in a laboratory. Thus, it can be applied easily to growing various thin films.

ACKNOWLEDGEMENTS

This research was supported by Basic Science Research Program through the National Research Foundation of Korea (NRF) funded by the Ministry of Education (NRF-2015R1D1A1A01060585).

SUPPORTING INFORMATION

Additional information as noted in the text. This information is available via the Internet at http://www.springer.com/chemistry/journal/11814.

REFERENCES

1. A. Mani, P. Aubert, F. Mercier, H. Khodja, C. Berthierd and P. Houdy, *Surf. Coatings Technol.*, **194**, 190 (2005).
2. X.-H. Gao, Z.-M. Guo, Q.-F. Geng, P.-J. Ma and G. Liu, *Solar Energy Mater. Solar Cells*, **157**, 543 (2016).
3. C. Zhao, Q. Wang, H. Zhang, S. Passerini and X. Qian, *ACS Appl. Mater. Interfaces*, **8**, 15661 (2016).
4. H. O. Pierson, Handbook of Chemical Vapor Deposition, Noyes Publications, Park Ridge, NJ (1999).
5. J. Rohrer and P. Hyldgaard, *Phys. Rev. B*, **82**, 045415 (2010).

6. M. A. Lieberman and A. J. Lichtenberg, Principle of Plasma Discharges and Materials Processing, Wiley, NY (1994).
7. A. Fridman, Plasma Chemistry, Cambridge University Press, New York, NY (2008).
8. H. T. Kim, C. D. Kim, M. S. Pyo and C. Park, *Korean J. Chem. Eng.*, **31**, 1892 (2014).
9. H. T. Kim, D. K. Park and W. S. Choi, *J. Korean Phys. Soc.*, **42**, S916 (2003).
10. H. T. Kim, M. J. Kim and S. H. Sohn, *J. Phys. Chem. Solids*, **73**, 931 (2012).
11. H. T. Kim and S. H. Sohn, *Vacuum*, **86**, 2148 (2012).
12. N. M. Shinde, R. J. Deokate and C. D. Lokhande, *J. Anal. Appl. Pyrolysis*, **100**, 12 (2013).
13. L. Chen and C. Park, *Korean J. Chem. Eng.*, **34**, 1187 (2017).
14. M. Qian and F. H. Froes, Titanium Powder Metallurgy: Science, Technology and Applications, Butterworth-Heinemann, Waltham, MA (2015).
15. H. T. Kim, T. Mun, C. Park, S. W. Jin and H. Y. Park, *J. Power Sources*, **244**, 641 (2013).
16. P. L. Huston, Chemical Kinetics and Reaction Dynamics, McGraw-Hill, New York, NY (2001).
17. R. B. Fair, Rapid Thermal Processing, Academic Press, Boston, MA (1993).
18. S. Adachi, The Handbook on Optical Constants of Metals: In Tables and Figures, World Scientific, Singapore (2013).

Supporting Information

Effects of growth temperature on titanium carbide (TiC) film formation using low-frequency (60 Hz) plasma-enhanced chemical vapor deposition

Hong Tak Kim*, Sung-Youp Lee, Hyeong-Rag Lee**, and Chinho Park*,†**

*School of Chemical Engineering, Yeungnam University, Gyeongsan 38541, Korea
**Department of Physics, Kyungpook National University, Daegu 41566, Korea
(*Received 23 May 2017 • accepted 5 September 2017*)

The XPS peaks related to oxygen were observed in the rage from 528 to 535 eV. The peak below 530 eV was attributed to the lattice oxygen, while peaks above 530 eV were related to chemical adsorption or carbon contaminations by organic materials. In this study, XPS peaks were positioned at approximately 530.4 eV and 531.6 eV, and this meant that oxygen component in TiC films originated from surface adsorption or contaminations. In addition, the XPS measurement was very sensitive to the surface of the films (skin depth: few nm). Therefore, the peak related to the oxygen can be exaggeratedly expressed compared to bulk oxygen component.

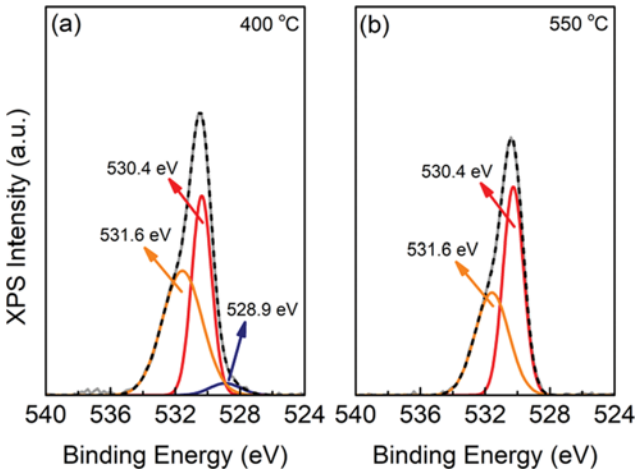

Fig. S1. XPS spectra of O 1s for the TiC films formed at (a) 400 °C, and (b) 550 °C.